Geometrical Mesh Improvement Properties of Delaunay Terminal Edge Refinement

A Progress Report

Technical report : CS-2006-16
The David Cheriton School of Computer Science
University of Waterloo ; Waterloo, Ontario, Canada, N3L 3G1

July 25, 2006

Bruce Simpson* and Maria-Cecilia Rivara†

July 25, 2006

Abstract

The use of edge based refinement in general, and Delaunay terminal edge refinement in particular are well established for planar meshing, but largely on a heuristic basis. In this paper, we present a series of theoretical results on the geometric mesh improvement properties of these methods. The discussion is based on refining a mesh to meet a specified angle tolerance.

1 Introduction

Delaunay terminal edge refinement, specified in §2, is a member of the family of edge-based adaptive mesh refinement methods; references to which follow in this introduction. These methods typically have a goal of generating a mesh appropriate to a piecewise linear approximation task for a region, D. However, in this report, we consider a geometric goal of producing a mesh in which the angles in every triangle exceed a specified minimum angle tolerance, $angTol$. This geometric goal can be related to what are termed mesh quality issues for piecewise linear approximation, see Berzins, [1] or Shewchuk, [26]. However, the connection between geometric goals and error control goals for piecewise linear approximation is complex, and we do not review it here.

Iterative refinement methods produce meshes for D that meet the angle criterion by starting with a coarse mesh for D that does not meet it and incrementally improving it by adding vertices until the criterion is met. We show a small example in Figure 1. Figure 1A shows an initial mesh for D. It has three triangles with small angles which reflect the presence of two small geometric details of D; the short boundary edge between vertices 2 and 3, and the narrow neck between

*School of Computer Science, University of Waterloo, Waterloo, Ontario, Canada, N2L 3G1 rbsimpson@uwaterloo.ca

†Department of Computer Science, Universidad de Chile, Blanco Encalada 2120, Santiago, Chile, mcrivara@dcc.uchile.cl

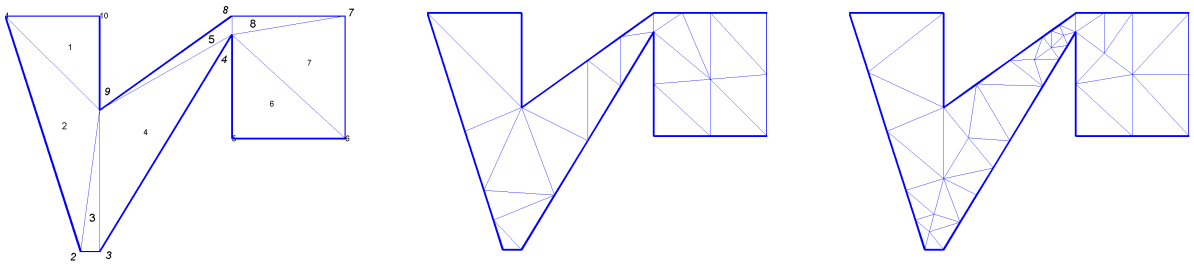

A - initial mesh B - $angTol = 20°$: 24 vertices C - $angTol = 30°$: 40 vertices

Figure 1: Simple example of Delaunay terminal edge refinement for angle control

vertices 4 and 8. Figures 1 B and C show meshes produced by Delaunay terminal edge refinement for $angTol = 20°$ and $30°$, respectively.

Edge based Delaunay refinement methods have been demonstrated to perform well in practice, as reviewed below. But they are largely heuristics in the sense that there is little in the way of formal proofs of their effectiveness. In this paper, we analyse a series of mesh improvement properties of these methods.

Delaunay terminal edge refinement is one of a class of iterative methods that create a sequence of Delaunay meshes, $\{M_n\}$, by inserting one vertex at a time. Here is a brief abstraction of one iterative step of the method.

1) Select t in M_{n-1} such that a smallest angle of $t < angTol$.

2) Use a longest edge propagation path from t to find a terminal edge of M_{n-1}, $e(t)$ that is close to t. (See §2.2 for these concepts.)

3) Let P be the midpoint of $e(t)$.
   if $e(t)$ is not a boundary edge then
      if P lies in the diametral circle of a boundary edge, e'
        then reassign P to be the midpoint of e'
      end if
   end if (1)

4) Delaunay insert P into M_{n-1} to produce M_n

We will often abbreviate 'Delaunay terminal edge refinement' to 'Deter' in the sequel; this will refer to one step of the iterative method as described by (1).

When a new vertex, P,is inserted into M_{n-1} to produce M_n in substep 4) of (1), a large part of M_{n-1} , $\bar{M}$, is unchanged; i.e. there submeshes CM_{n-1} and BM_n such that $M_{n-1} = \bar{M} + CM_{n-1}$ and $M_n = \bar{M} + BM_n$[1] In this paper, we study the angle properties of BM_n for Delaunay terminal edge refinement. Since the goal of the refinement method is to produce a mesh that meets a minimum angle size criterion, it would desireable if the smallest angle in the triangles of BM_n were

[1]In the terminology of George and Borouchaki, [4], CM_{n-1} is the cavity of P and BM_n is the ball of P.

larger than the smallest angle in CM_{n-1}. However, as this report details, for Delaunay terminal edge refinement, there are worst cases in which this does not happen. We show that it is possible that one angle in BM_n is smaller than the minimum angle of CM_{n-1}; this worst case can occur only for a special configuration of CM_{n-1}. While it appears to us that this configuration cannot be reproduced indefinitely, we have not studied the implications rigorously.

We conceptualize substep 4) of (1) as consisting of a longest edge bisection of the triangles incident on the edge bisected by P, followed by a conversion of the resulting mesh to a Delaunay mesh, if necessary. This allows us to analyse the new angles created for the mesh in an orderly way. For an arbitrary triangle, t, the longest edge bisection of t is the splitting of t into two triangles (t_A, t_B) by joining the midpoint of a longest edge to the opposite vertex. In the sequel, 'longest edge bisection' will often be abbreviated as 'LEBis'. For angle improvement, the intuitive view of a LEBis is that the child triangle t_A is no improvement over t, while t_B is better than t. In §2, we quantify this intuitive viewpoint. t_A retains the smallest angle of t, which we denote by $\alpha_0(t)$. In the worst case, t_A can have a new angle smaller than $\alpha_0(t)$. We provide some lower bounds for the size of this angle. We also show the configurations in which t_B can be a well shaped triangle; it cannot have an angle smaller than $min(\alpha_0(t), \pi/6)$.

In Delaunay terminal edge refinement, LEBis is limited to special edges in the mesh referred to as 'terminal edges'. In §2.2, we review the concept of terminal edges and details of terminal edge refinement and present some implications for angles in the triangles to be refined that result from its use.

In §3, we discuss the implications of Delaunay insertion for the insertion point determined as discussed in §2. This process is central to removing small angles from the mesh. If $\alpha_0(t)$ is less than $angTol$, then the LEBis analysis of t in §2 shows that this angle is inherited by t_A. So, if an angle of this size is not to appear in BM_n, it must result from the conversion of the mesh created by LEBis to a Delaunay mesh. In §3.1, we discuss the improvements that follow from this conversion. However, in the worse case, the improvement can be arbitrarily small. We present a precise characterization of the worst case. In §3.3, we apply some of the ideas developed earlier to analyze a special configuration and demonstrate a lower bound on the edge lengths that can result from this configuration under subsequent refinements.

Edge based refinement methods for 2 and 3 dimensions have a relatively long history. Perhaps the earliest reference to adaptive refinement based on LEBis is Sewell, 1979, [24]. See also Bank and Sherman[2] , 1979, [23]; subsequent references are Bank, 1998 [6] , Rivara et al, 1994 - 1997, [7, 8, 20, 9, 13, 15], Nambiar et al, 1993, [12], Muthukrishnan et al, 1995, [11], Morin et al, 2002, [10]. More recently, the observation that the constrained Delaunay triangulation (CDT) provides the triangulation of a set of vertices that is the most 'improved' with regard to angles has lead to using refinement methods that produce a sequence of CDTs, i.e. Delaunay refinement methods. The combination of edge refinement and Delaunay insertion has been described by George and Borouchaki , 1997, [5, 4] and Rivara and her collaborators, 2000 - 2002 [17, 18, 27]. Strong mesh improvement properties for Delaunay **circumcenter** based refinement were established by 1993 by Chew, 1993, [3], Ruppert, 1995 [16], and Shewchuk, 1996 [25]. In particular, under appropriate conditions on D, the methods are guaranteed to produce meshes with all angles $> angTol$, for a significant range of $angTol$. Applications of this form of refinement have been described by Weatherill et al ,1994, [33, 34] and Baker, 1989, [21]. Baker also published a comparison of edge

[2]The edge based refinement of this reference is not exactly LEBis.

base and circumcenter based refinement, 1994, [22].

At the time of this report, we have still many unanswered questions about the theory of Delaunay terminal edge refinement. In this sense, the report is a progress report for on-going research.

2 Components of Delaunay terminal edge refinement (Deter)

In this section, we present properties of triangles that result from a simple longest edge bisection. The LEBis of t splits t into two child triangles, t_A and t_B as described in §2.1. If t is a triangle with a small angle, then, intuitively, this split isolates the unwanted small angle feature in t_A, leaving an improved triangle t_B. In §2, we quantify these roles of t_A and t_B. In §2.1, we start with a comprehensive study of the angle properties of t_A and t_B.

As mentioned in the introduction, LEBis is introduced into our discussion to help us to analyse the angle implications of the refinement. Algorithmically, the refinement amounts to the Delaunay insertion of the midpoint of the terminal edge selected for refinement, which can be accomplished several ways.

In §2.2, we explain the components of Deter refinement and our terminology for them. We then present two bounds on the angles in the pairs of triangles incident on a Delaunay terminal edge. In Corollary 2.1 and its discussion, we present important conditions for the removal of small angles from the mesh.

One of the properties of LEBis of §2.1 is that if t is an acute triangle, then t_A has an angle that is smaller than the smallest angle in t. In §2.3, we provide bounds on how small this new angle can be.

In §2.4, we study the extent to which t_B is an improvement relative to t. A table of improvement cases is given; the worst case of 'improvement' is identified and well defined. In this worst case, t_B has the same smallest angle size as t, but a better shape for further refinement.

2.1 Basic properties of longest edge bisection of triangles - LEBis

Individual properties of LEBIS have been reported in a variety of references, [20, 15, 19]. In this subsection, we believe we have included all previously published properties, provided some simpler proofs for some cases, and added new properties in Theorem 2.1 b) and c) and Theorem 2.2.

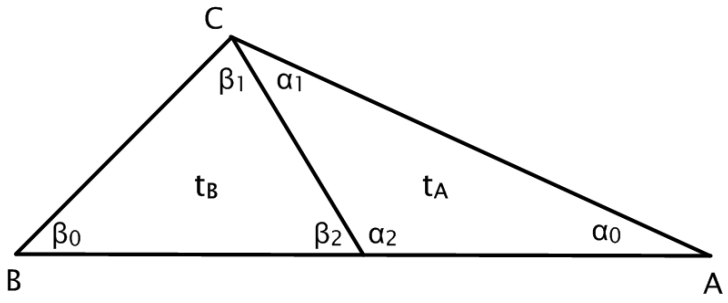

Figure 2: notation for longest edge bisection

We standardized the notation for this splitting by labeling the vertices of t as A, B, C and

normalizing this labeling by requiring

$$|B-C| \leq |C-A| \tag{2}$$
$$|C-A| \leq |B-A| \tag{3}$$
$$M = (A+B)/2$$

where M is the midpoint of the longest edge that is to be split. These determine the labels A, B and C uniquely, if t has only one longest edge. In Figure 2 we show this labelling for a clockwise ordering of ABC. In this figure, we have labelled the two new child triangles, t_A and t_B; their indices reflect their incidence on vertices A and B respectively. We have also labelled the angles of t_A (t_B) as α_j (β_j) ; for $j = 0, 1, 2$. α_0 and β_0 are inherited unchanged from t.

The following lemma and theorem present some simple properties of a LEBis of any t.

Lemma 2.1 *Each of the assertions in the following groups is equivalent to any other in the group.*

a)	*b)*	*c)*
t is a right angled triangle	*t is an acute triangle*	*t is an obtuse triangle*
$\alpha_1 = \alpha_0$	$\alpha_1 < \alpha_0$	$\alpha_1 > \alpha_0$
$\beta_1 = \beta_0$	$\beta_1 < \beta_0$	$\beta_1 > \beta_0$
$\|A-M\| = \|C-M\|$	$\|A-M\| < \|C-M\|$	$\|A-M\| > \|C-M\|$

Proof These equivalences follow from the basic geometry of triangles, plus the sine law applied to t_A , i.e.

$$\frac{|C-M|}{sin(\alpha_O)} = \frac{|A-M|}{sin(\alpha_1)} = \frac{|A-C|}{sin(\alpha_2)}$$

and t_B. For assertion group a), note that $CC(t)$ is the diametral circle of edge AB from which the various assertions follow. □

Theorem 2.1 *The following angle bounds apply*

a) $\alpha_1 \geq \alpha_0/2$

b) $\beta_1 \geq \pi/6$

c) $\beta_1 \geq \alpha_1$

d) $\beta_2 \geq 3\alpha_0/2$

Proof Assertion a) follows from the following strong result due to Rosenberg and Stenger [35]: For any triangle t^* obtained in the iterative bisection process, the smallest angle of t^* is greater than or equal to $\alpha_0/2$.

For assertion b), Figure 3 shows the circle of radius $|B-A|$ centered on A. Let $C(\alpha_0)$ be the point at which line segment on the edge AC of t meets this circle. Note that since α_0 is a smallest angle of t, $\alpha_0 \leq \pi/3$. Let $\beta_1(\alpha_0)$ be the angle $BC(\alpha_0)M$; then $\beta_1(\alpha_0) < \beta_1$. The triangle $BAC(\alpha_0)$ is isosceles, so if we denote its angle at B by $\beta_0(\alpha_0)$ we have

$$\beta_0(\alpha_0) = \pi/2 - \alpha_0/2; \;\; |C(\alpha_0) - B| = 2|B-A|sin(\alpha_0/2). \tag{4}$$

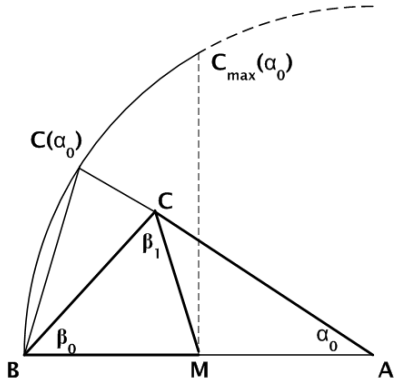

Figure 3: Bound on β_1

So the sine law for triangle $BC(\alpha_0)M$ implies

$$\frac{sin(\beta_1(\alpha_0))}{|B-A|/2} = \frac{sin(\beta_0(\alpha_0))}{|C(\alpha_0)-M|}$$

and consequently

$$sin(\beta_1(\alpha_0)) = (\frac{|B-A|/2}{|C(\alpha_0)-M|})\, cos(\alpha_0/2). \tag{5}$$

Both terms in the product on the right hand side of (5) are monotone decreasing in α_0, so $sin(\beta_1(\alpha_0)) > sin(\beta_1(\pi/3))$. Consequently

$$\beta_1 \geq \beta_1(\alpha_0) \geq \beta_1(\pi/3) = \pi/6$$

Assertion c) probably follows from a simple geometric observation; but we support it using the sine laws for t_A and t_B; i.e.

$$\frac{sin(\beta_1)}{|B-M|} = \frac{sin(\beta_0)}{|C-M|} \geq \frac{sin(\alpha_0)}{|C-M|} = \frac{sin(\alpha_1)}{|A-M|}$$

Assertion d) follows from $\beta_2 = \alpha_1 + \alpha_0$ and using a) of this theorem and b) of Lemma 2.1. □

Theorem 2.2 *The following angle bounds apply conditionally*

a) if t is obtuse, then $\beta_2 \geq 2\alpha_0$

b) if t is acute, then t_B is acute

c) if $\alpha_0 < \pi/6.215$, or t is obtuse and $\alpha_0 < \pi/6$ then $\beta_1 > min(\beta_0, \beta_2)$

d) if $\alpha_0 > \arcsin(1/3) = 19.5^\circ$, then $\beta_1 < \pi/2$, i.e. t_B is acute.

For a), we again note that $\beta_2 = \alpha_1 + \alpha_0$ and use $\alpha_1 > \alpha_0$ for obtuse triangles as per Lemma 2.1.

For b), let $circ1$ be the diametral circle of BA, and let $circ2$ be the diametral circle of BM, which is contained in $circ1$. t acute implies $C \notin circ1$, so that $C \notin circ2$ and consequently, t_B is acute.

For c) , we will show that under the conditions on α_0 and t, then edge BM of triangle t_B is not its shortest edge. Let C_1 and C_2 be two circles of radius $|B - M|$. C_1 is centered on M, and is the diametral circle of edge AB; C_2 is centered on B. If C lies inside either one, then edge BM is not the shortest edge of t_B and so $\beta_1 > min(\beta_0, \beta_2)$ as stated in b). We demonstrate two ways this can happen. First consider C_1 and let Z be the intersection point of C_1 and C_2 which lies above edge AB. Then triangle BMZ is equilateral, and angle $BAZ = .5$ angle $BMZ = \pi/6$ since both these angles are subtended by the chord BZ with M at the center of the circumcircle of BAZ. So, if $\alpha_0 < \pi/6$ and t is obtuse, so that C in in C_1, then edge CM is shorter than edge BM in t_B.

However, the line AZ is tangent to C_2 at Z. This can be seen from the facts that triangle ZMA is isosceles , so that angle $MZA = \pi/6$, and angle $BZA =$ angle $BZM +$ angle $MZA = pi/2$. If t is acute and $\alpha_0 = \pi/3$, then C lies outside C_2, as well as outside C_1, and BC is longer than edge BM. Consider the point P where C_2 intersects the circle of radius $|A - B|$ centered on A. C must lie on the line segment AP since AB is a longest edge ot t. The triangle BAP is isosceles, with base $= |P - B| = |A - B|/2$. Consequently, angle $BAP = \text{asin}(.25) > \pi/6.215$. Hence, if $\alpha_0 < \pi/6.215$, then edge BM is longer than the minimum of the other two edges of t_B, regardless of the shape of t.

For d), let M' be the midpoint of edge BM, and let C' be the point on the diametral circle of edge BM' at which the tangent to this circle through A touches the circle. Let $\bar{\alpha}$ be the angle MAC' at A made by this tangent. Then, since angle $AC'M' = \pi/2$,

$$sin(\bar{\alpha}) = |M' - C'|/M' - A| = 1/3$$

If $\alpha_0 > \bar{\alpha}$ then C must lie outside this diametral circle and t_B is acute. Evidently, this condition is sufficient, but not necessary. □

2.2 Delaunay terminal edges and triangle configurations

For a planar mesh, a boundary edge is terminal if it is the longest edge of its incident triangle and an internal edge is terminal if it is the longest edge of each of the two incident triangles. Figure 4 (a) shows edge AB as an example of an internal terminal edge and Figure 4 (b) shows edge CD as a boundary terminal edge. These figures show sequences of triangles $\{t_k\}, k = 0, 1, 2, 3$ such that the shared edge of t_k and t_{k+1} is a longest edge of t_k but not t_{k+1} for $k = 0, 1$ (and for (b), for $k = 2$).a These are examples of longest edge propagation paths for t_0 in each case. In general, they are of arbitrary length. We will abbreviate 'longest edge propagation paths' for t_0 as 'Lepp(t_0)'. Lepp, and the terminal edge concepts, were introduced and used in references [15, 19, 20].

We present two motivations for the concept of terminal edges. The first motivation is that one of the tactics in refinement for geometric improvement is to refine the largest triangles first. A terminal edge in a mesh is a local maximum for edge length in a graph sense so it is a good candidate for refinement.

The second motivation is more fundamental. Consider two neighbouring triangles t_k, t_{k+1} as shown in Figure 4 (a) for $k = 0, 1, 2$. For $k = 0, 1$, a refinement of the mesh could be made by

splitting t_k and t_{k+1}, using the midpoint of their common edge. This splitting would be a LEBis of t_k, but not t_{k+1}. However, for $k = 2$, terminal edge AB is a longest edge of both t_2 and t_3, so the midpoint refinement is a LEBis of both triangles.

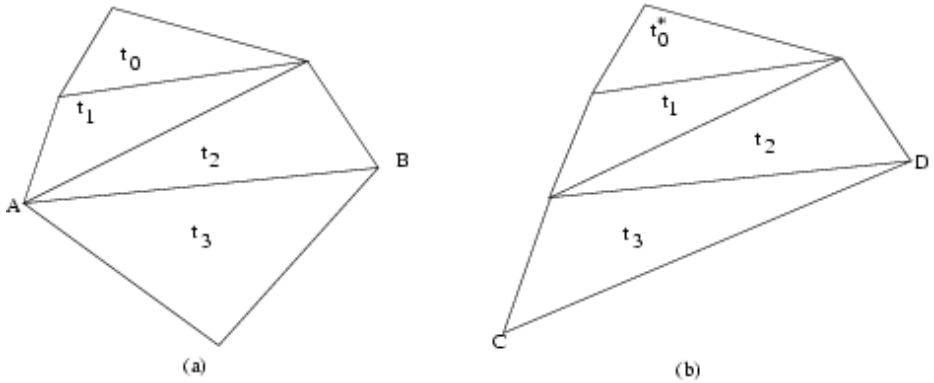

Figure 4: Sequences of mesh triangles; common edge of t_k, t_{k+1} is a longest edge of t_k

Terminology and its concepts

We now explain the terminology of the paper. Terminal edge bisection is a refinement technique in which a terminal edge is identified in each refinement step, and its midpoint inserted into the mesh by simple LEBis of each incident triangle as described in §2.1 above. Delaunay terminal edge bisection is is a modification of terminal edge bisection in which the meshes being refined are Delaunay, or constrained Delaunay, and the insertion is a Delaunay point insertion. Given a triangle, t_0 that is to be refined, the algorithm for computing a longest edge propagation path starting at t_0 locates a terminal edge near t_0, in a graph sense. Figure 4 illustrates this concept for the two triangles marked t_0 on the left and t_0^* on the right.

Finally, Deter of a triangle t will refer to finding a terminal edge associated with t using Lepp and performing Delaunay terminal edge bisection on it. As the examples of Figure 4 show, Deter of t may not modify t, in which case the process can be repeated in the refined mesh. Evidently, this repeated application of Deter to t must terminate and modify t either by Delaunay terminal edge bisection of its longest edge, or by swapping it during the Delaunay insertion of some other midpoint. Algorithmic details of Deter, including repeated application to a given t, are given in [15, 19, 20, 27]

Our description of one step of Deter at (1) includes a 'encroachment' rule when the midpoint of a terminal edge is inside the diametral circle of some boundary edge, not necessarily terminal. Such rules are needed to ensure mesh improvement by refining boundary edges, [3, 16]. As the small examples of Figure 1 of the introduction show, the insertion of boundary vertices plays a very important role in computing a mesh that meets a minimum error tolerance. Nevertheless in this report, we will restrict our attention to refinement of terminal edges.

Configurations of terminal triangles

Let t_1, t_2 be the two neighbouring triangles on an internal terminal edge, AB. Simple bisection of AB results in 4 new triangles in the mesh, which we can designate by $t_{j,A}$ and $t_{j,B}$ for $j = 1, 2$, as in the previous subsection, §2.1. If t_j are both acute, the the discussion of $t_{j,A}$ and $t_{j,B}$ in §2.1 applies independently for $j = 1, 2$. For a pair of triangles (t_1, t_2) sharing a Delaunay edge, the sum of the angles opposite the common edge cannot exceed π, consequently, at most one of the t_k can be obtuse. In this case, there are restrictions on the t_j that we describe in this subsection using Figure 5. The figure shows only t_1; we denote the vertex of t_2 opposite edge AB, which is

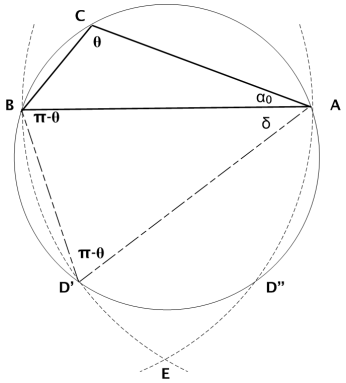

Figure 5: The configuration of triangles at an internal terminal edge

not shown, by D. The dashed circular arcs are part of the circles of radius $|B - A|$ centered at A and B respectively and the circumcircle of t_1 is shown with a solid perimeter. Because edge AB is terminal and the triangles are Delaunay, D must lie in the small region at the bottom of the diagram below the arc of $CC(t_1)$ between D' and D'' and inside the two dashed arcs that meet at E. One implication of this configuration is the following theorem.

Simple implications of this diagram are the following lemma and corollary.

Lemma 2.2 *For any pair of Delaunay terminal-triangles t_1, t_2 sharing an internal terminal edge, largest angle(t_i) $\leq 2\pi/3$ for $i = 1, 2$.*

Proof: Assume the largest angle occurs in obtuse triangle t_1 as shown in Figure 5. If $\theta > 2\pi/3$, then E lies inside $CC(t_1)$, which is impossible. □

Corollary 2.1 *For a LEBis of tin a Delaunay mesh, if $\alpha_0 + \alpha_1 < \pi/3$ then edge CA is not a terminal edge. Note $\alpha_0 + \alpha_1 = \beta_2$.*

Basically this corollary shows that if t_A is a 'skinny' obtuse triangle, then CA cannpt be a terminal edge. There are many special configurations that ensure $\alpha_0 + \alpha_1 < \pi/3$; i.e. t is acute and $\alpha_0 < \pi/6$, or t is obtuse and $\alpha_1 < \pi/6$.

The following theorem shows that if the edge is a terminal edge, then the more obtuse t_1 is, the larger the smallest angle of acute t_2 is.

Theorem 2.3 *Let t_1 and t_2 be incident on an internal terminal edge and let θ be the largest angle of t_1. Let $\alpha_0(t_2)$ be the smallest angle of t_2. If $\pi/2 \leq \theta \leq 2\pi/3$,*

$$\alpha_0(t_2) \geq 2\theta - \pi$$

Proof: Referring to Figure 5, vertex D of t_2 must be inside the lens of dashed arcs and outside the circumcircle of t_1. D', D'' are the points where the lens intersects $CC(t_1)$. Assume that a smallest angle of t_2 is at A. Let δ be the angle BAD'; then $\alpha_0(t_2) > \delta$. Look at triangle $BD'A$. Because C, B, D', A are co-circular, the opposite angles in this quadrangle add to π and so angle $BD'A$ is $\pi - \theta$ as marked. But because B and D' are on the dashed arc centered at A, triangle $AD'B$ is isosceles and angle $D'BA = \pi - \theta$ as marked. So $\delta = 2 * \theta - \pi$. □

This theorem, and Figure 5 illustrate restrictions on the configuration of triangles that share a terminal edge, e.g. if $\theta = 7\pi/12$, then $\alpha_0(t_2) \geq \pi/6$.

As mentioned at the outset of this section, one of the characteristics of LEBis is that it necessarily produces an obtuse child triangle, t_A, which retains angle α_0 from its parent,t and, if t is acute, has a smaller angle α_1. So, if α_0 is small, mesh improvement in the sense of removing small angles must come from subsequent processing of t_A. It may happen that the Delaunay insertion of M removes t_A from the mesh. The implications of of this possibility are discussed in the next section. If not, i.e. if edge AC is an internal Delaunay edge , it may not be a terminal edge. Intuitively, it would be expected that the configurations of the two triangles incident on edge AC would not commonly meet the conditions presented above for it to be a terminal edge, in general. Corollary 2.1 is a particular instance of this. So, in general, it would be expected that repeated Deter refinements of t_A would, sooner or later, result in edge AC being removed from the mesh by a Delaunay insertion following the bisection of some other nearby terminal edge.

2.3 Bounds on the size of α_1 for acute t

Here, we next discuss some bounds on the size of α_1 in the case that t is an acute Delaunay terminal triangle.

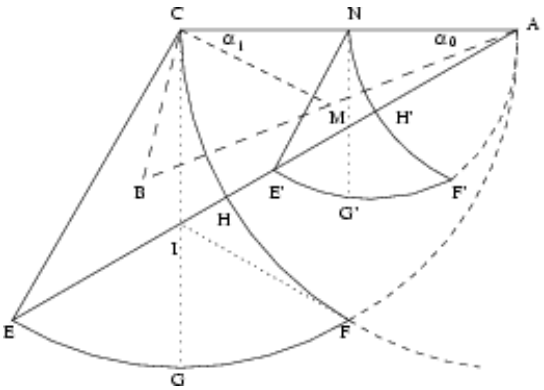

Figure 6: Regions EFC and E'F'C' are geometrical places for vertex B and midpoint M for a terminal triangle BAC with respective smallest and largest angles of vertices A and C

Figure 6 shows the possible locations for vertex B of a Delaunay terminal triangle for a fixed second longest edge CA. It also shows the possible locations for M. It supports an analysis of

properties of t_A and t_B as parametrized by B. Since BA is the longest edge, the following two conditions hold: Condition (2) constrains B to lie inside the circular arc EFA of centre C and radius $|C-A|$. Consequently, M lies inside the circular arc $CF'A$ of centre $N=(C+A)/2$ and radius $|C-A|/2$. Condition (3) constrains B to lie outside the circular arc CF of centre A and radius $|C-A|$, and so M lies outside circular arc NF' of centre A, radius $|C-A|/2$. The line CE makes an angle of 120° with CA; this constraint is a direct application of Theorem 2.1 for an unconstrained Delaunay terminal triangle.

Some of the properties of the triangles of the diagram are summarized in the table given below. We shall denote by the smallest and largest angle of any triangle t by θ_{min}(t) and θ_{max}(t) respectively.

B is in/on	property
edge CE	$\theta_{max}(t) = 120°$
arc EF	t is an isosceles triangle with smallest edge equal to second longest edge
arc CF	t is an isosceles triangles with longest edge equal to second longest edge
edge CG	t is a right triangle, $\alpha_0 = \alpha_1$, $\theta_{min}(t_A) = \alpha_0 = \alpha_1$
interior of region CEG	$\alpha_1 > \alpha_0$, $\theta_{min}(t_A) = \alpha_0$
interior of region CGF	acute triangles with $\alpha_1 < \alpha_0$, $\theta_{min}(t_A) = \alpha_1$

Item a) of Theorem 2.1 is quite a weak lower bound for α_1 when α_0 is small. By studying the distribution of angles (α_0, α_1) as shown in the diagram of Figure 7, we can see the distribution of the ordered pair of angles (α_0, α_1). Figure 7 is a relabelled version of Figure 6. In Figure 7, the

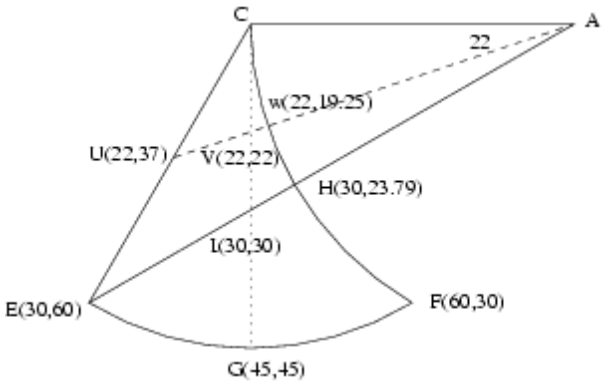

Figure 7: Distribution of angles (α_0, α_1) for a terminal triangle with B in CEF

segments EH and UW respectively correspond to the terminal triangles with smallest angles equal to 30° and 22°. Note for $\alpha_0 = 30°$, the angle α_1 decreases from 60° to 23.79° along EH, while for $\alpha_0 = 22°$ the α_1 angle decreases from 37.75° to 19.25° along UW. Remember that segment line CG indentifies right terminal triangles with $\alpha_0 = \alpha_1$. Note also that the ratio α_0/α_1 increases along

line segment E to C and arc F to C.

We consider the case $\alpha_0 = 22^\circ$ since we are interested in improvement of angles in the mesh below this value (see section 3.1 for an explanation of this constraint).

These properties and continuity reasoning allows to state the following lemma:

Lemma 2.3 *a) For acute terminal triangles with smallest angle $\alpha_0 \leq 30^\circ$ (B in region CIH), it holds that $\alpha_1 \geq 0.79\alpha_0$.*

b) For acute terminal triangles with smallest angle $\alpha_0 \leq 22^\circ$ (B in region CVW), it holds that $\alpha_1 \geq 0.886\ \alpha_0$.

c) For acute terminal triangles the ratio α_0/α_1 increases (α_1 approaching α_0) while α_0 decreases.

2.4 t_B is worst case safe

We now quantify the notion that the triangle t_B created by a LEBis of triangle t is a better triangle than t. The results of the preceding sections are used, and extended, to prove the following theorem about the smallest angle of $t_B\ = \alpha_0(t_B)$. This theorem also refers to the child triangle of a LEBis of t_B that retains angle $\alpha_0(t_B)$ which we could denote by $t_{B,A}$. More precisely, the theorem refers to the other acute angle of $t_{B,A}$, which we could denote by $\alpha_1(t_{B,A})$. However, this seems unnecessarily clumsy, so we will simply denote it by $\alpha_1(t_B)$. An example is shown in Figure 9. Note that the vertex at which $\alpha_0(t_B)$ occurs is opposite to the shortest edge of t_B, which depends on the location of C as listed in Table 1 below.

Theorem 2.4 *For any triangle t in mesh M,*

$$\alpha_0(t_B) \geq min(\alpha_0(t), \pi/6) \tag{6}$$

and if t_B is acute

$$\alpha_1(t_B) \geq min(1.4 * \alpha_0(t), \pi/6) \tag{7}$$

Essentially, this theorem says that in the worst case, the creation of t_B by LEBis of t and subsequent conversion of the new mesh M to a Delaunay mesh cannot produce any new angles that are smaller than the smallest angle in t, or 30°. The case that $\alpha_0(t_B) = \alpha_0(t)$ occurs if t is isosceles with $\beta_0 = \alpha_0$. The theorem shows that this is the worst possible case, and, the proof shows that it is the only way that $\alpha_0(t_B) = \alpha_0(t)$ if $\alpha_0(t) \leq \pi/6$.

Proof : Figure 8 shows:

- the longest edge AB of t for bisection,
- its midpoint, M, and its quarter point Q midway between B and M
- three related circular arcs:

  arc BEH is part of the circle centered at A of radius $|B - A|$. C must lie above BM, on, or to the left of, MH, and to the right of arc BEH.

  arc BFG is part of the circle centered at M of radius $B - M$

  arc MFE is part of the circle centered at B of radius $B - M$.

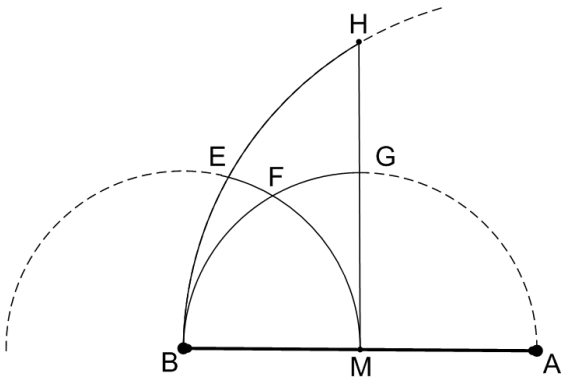

Figure 8: Regions for C

- evidently, F is the intersection of arcs BG and ME

The proof of the theorem involves examining the cases arising from the different regions of domain in which C can lie. We summarize these cases in Table 1.

Region for C	t is	lower bound	shortest edge	lower bound
		for $\alpha_0(t_B)$	of t_B	for $\alpha_1(t_B)$
EFGM	acute	$\pi/6$	BM	$\pi/6$
EBF	acute	$1.5\alpha_0(t)$	BC	$1.4\alpha_0(t)$
BQF	obtuse	$1.5\alpha_0(t)$	BC	-
QFGM	obtuse	$\alpha_0(t)$	CM	-

Table 1: Lower bounds for $\alpha_0(t_B)$

The fourth column of this table implicitly indicates which of β_k is the smallest angle of t_B, $\alpha_0(t_B)$, since it is opposite the shortest edge of t_B. The entry in the third column for row EFGM follows because β_1 is a minimum for this region when C is at H. The next two entries in the third column follow from Theorem 2.1, and the bottom entry follows because $\beta_0(t) \geq \alpha_0(t)$ with equality only if C lies on MH.

The fifth column of the table is relevant for t_B acute because as Lemma 2.1 pointed out, for acute t_B, $\alpha_1(t_B) < \alpha_0 t_B$. Furthermore, as we detail in §3.1 below, and angle arbitrarily close to α_1 can created in the conversion of the refined mesh to a Delaunay mesh. The entry for EFGM in the 5 th column follows also because $\alpha_1(t_B)$ is minimized for C in region EFGM by $C = H$. The entry in the 5 th column for EBF is based on a somewhat complex explicit computation; we present stages of it in Lemma 2.4 and its corollary which follow. □

Lemma 2.4 *For acute isosceles t,*

$$sin(\alpha_1(t_B)) = (1/f)\, sin(\alpha_0(t))$$

for

$$f = 2(\,(sin^2(\alpha_0(t)/2) + 1/4)^2 + sin^2(\alpha_0(t)/2)/4\,)^{1/2} \tag{8}$$

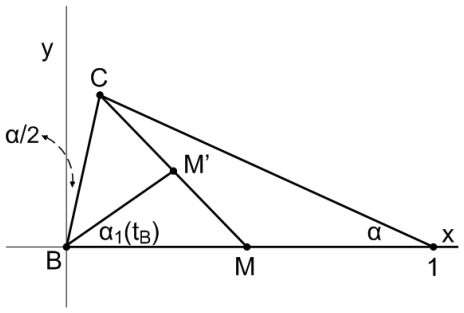

Figure 9: configuration of $\alpha_1(t_B)$ for acute, isosceles t

Proof : Figure 9 shows the LEBis of acute isosceles t with edge AB scaled to length 1. $|B-C| = 2sin(\alpha/2)$ and, in the coordinate system shown, $C = (2sin^2(\alpha/2), sin(\alpha))$ where we abbreviate $\alpha_0(t)$ to simply α. The longest edge of t_B is CM , where the coordinates of M are $(1/2, 0)$, and the smallest angle is $CMB = \beta_2(t)$. So LEBis of t_B will introduce the midpoint of line segment $CM = M'$ into the mesh, with $\alpha_1(t_B)$ as angle $M'BM$. The coordinates of M' and be computed as $(sin^2(\alpha/2) + 1/4, sin(\alpha)/2)$ from which the lemma follows. □

Corollary 2.2 *For acute t with $\alpha_0(t) \leq \pi/6$,*

$$sin(\alpha_1(t_B)) \geq 1.45 sin(\alpha_0(t))$$

For C in EFB of Figure 8, we can see that $\alpha_0(t) \leq \pi/6$ and that for given $\alpha_0(t)$, the worst case of bounding $\alpha_1(t_B)$ below by $\alpha_0(t)$ occurs for acute isosceles t. The factor, f of Lemma (2.4) is monotone increasing in α and for $\alpha = \pi/6$, $f = .68477$.

3 Geometric mesh improvements: internal terminal edges

The previous section discussed the angles generated by LEBis of a boundary terminal triangle, t_1, or a pair of triangles, t_1 and t_2 which share an internal terminal edge. We noted that the child triangles $t_{j,B}$, $j = 1$ or $j = 1, 2$ usually had larger angles, and in any case, were no worse, than t_j. However, the other child triangles $t_{j,A}$ were definitely not improved, and if t_j is acute, then $t_{j,A}$ has an angle smaller than $\alpha_0(t_j)$. rIn the introduction, we described the n the step of iterative Deter as the replacement of submesh CM_{n-1} of M_{n-1} by submesh BM_n of M_n. Conceptually, we view the creation of M_n as talking place in 2 stages. The first is the insertion of midpoint M into mesh M_{n-1} by LEBis of the t_j. We will denote the resulting mesh by M_{SB}. In general, M_{SB} is not Delaunay, so the second stage is the conversion of M_{SB} to M_n. I.e.

$$M_{n-1} = \bar{M} + CM_{n-1} > M_{SB} > \bar{M} + BM_n = M_n$$

This provides the opportunity for removing small angles of $t_A \in M_{SB}$ from M_n if edge CA is not Delaunay in M_{SB}.

The conversion of M_{SB} to Delaunay is known to increase the minimum angle in BM_n. In Theorem 3.1, we add more precision to this general observation by identifying two vertices of BM_n

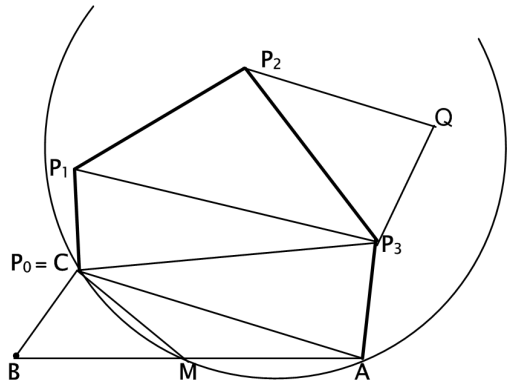

Figure 10: Example of the partial cavity of vertex M in mesh M_{SB} with $NA = 4$

that are influenced by α_0 and α_1 respectively. However, it may be that CA is a Delaunay edge in M_{SB} an so it also appears in M_n, along with angles α_0 and α_1. In this case, it is not likely that CA is a terminal edge, In §2, we presented two criteria for terminal edges, and Lemma 3.2 add a third. Basically they indicate that the longest edge of a triangle with two small angles cannot be a terminal edge. Since the LEBis stage of Deter is limited to terminal edges, if CA is not terminal, then its midpoint will not be inserted in the mesh and so any elimination of CA from the mesh must come when an insertion of the mipoint of some nearby terminal edge makes CA a non-Delaunay edge.

In §3.3, we present a special case of mesh non-degeneration, if not improvement, when CA is a Delaunay, but not terminal, edge.

3.1 Delaunay insertion of point M

To describe the conversion of M_{SB}, we will use the terminology of George and Borouchaki ,[4]. The cavity of the vertex M in M_{SB} is the set of triangles, t, such that $M \in \mathrm{CC}(t)$[3]. It has a polygonal boundary that is star-shaped with respect to vertex M. We will denote the boundary vertices of the cavity by P_k for $k = 0$, to N in clockwise order about M starting with $P_0 = C$. Since A, B and C are on this boundary, $N \geq 2$. The result of the Delaunay insertion of vertex M is that the triangles in the cavity of M are removed from M_{SB} and a new set of triangles appear in M_n with M as a vertex, i.e. the triangles MP_kP_{k+1}.

We let NA be the index of A in the list of boundary vertices of the cavity of M i.e. $P_{NA} = A$. The subset of the cavity of M that is bounded by the first $NA+1$ vertices and the edges AM and MC will be referred to as the partial cavity of M. An example is shown in Figure 10; this figure also shows $\mathrm{CC}(t_A)$ of triangle $t_A = CMA$ with the P_k in its interior. This illustrates the statement of the following lemma. We have also shown a mesh vertex, Q , and triangle P_2QP_3 which are not in the cavity of M although they are in $CC(t_A)$. So the converse of the lemma is not true.

Lemma 3.1 *If $NA > 1$, P_k is in $CC(t_A)$ for $1 < k < NA$*

[3] '$\mathrm{CC}(t)\equiv$ the circumcircle of t'

Proof C and A are not in $CC(P_{k-1}P_kP_{k+1})$. Consequently, if $M \in CC(P_{k-1}P_kP_{k+1})$ then $CC(P_{k-1}P_kP_{k+1})$ must cut the edge CA twice, at points C' and A' either at the endpoints of this edge or in its interior. The chord $C'A'$ of $CC(P_{k-1}P_kP_{k+1})$ cuts this circle into two sections; one contains M in its interior and the other contains P_k on its boundary. We will designate this latter section by $Cap(P_{k-1}P_kP_{k+1})$. By the symmetry of circumcircles, since M is inside $CC(P_{k-1}P_kP_{k+1})$, P_k is inside $CC(C'MA')$; in fact, in the section of $CC(C'MA')$ opposite to M across the chord $C'A'$. We will designate this section as $Cap(C'MA')$. Now, $Cap(C'MA') \subset Cap(t_A)$; so we have $P_k \in Cap(C'MA') \subset Cap(t_A) \subset CC(t_A)$.

We will study the angles and edge lengths of the new triangles incident on M. Let

$$\alpha_{min}(M) = \begin{array}{l}\text{the minimum angle of the triangles in the partial cavity of} \\ M \text{ excluding triangle } t_A\end{array} \tag{9}$$

Now, each triangle $t \in M_{SB}$ in the cavity of M has vertices, P_i, P_j, P_k for $i < j < k$. If t has an edge on the boundary of the cavity, then $i = j - 1$. In this case, $M \in \mathrm{CC}(t)$ implies that the angle at M in M_n opposite edge P_{j-1}, P_j is larger than the angle opposite edge P_{j-1}, P_j in t. So, in particular, the angle at M is larger than $\alpha_{min}(M)$. Intuitively, we can see that the closer a cavity edge, $P_{j-1}P_j$, is to M the larger this angle improvement will be. Conversely, if $\mathrm{CC}(t)$ is very close to $\mathrm{CC}(t_A)$ then very little angle improvement can occur.

BM_n is the set of triangles $P_jP_{j+1}M$ for $0 \le j \le NA - 1$; i.e. the set of triangles in M_n that replace the partial cavity of M. It follows immediately from the Delaunay mesh property of maximizing the minimum angle in a triangulation that the minimum angle of the triangles of BM_n is not less than the minimum angle of the triangles of the partial cavity of M. However, this is not a very insightfull observation. In particular, the partial cavity of M contains t_A from the longest edge bisection of t and the minimum angle of t_A can be α_1, which can be smaller than existing angles in the mesh. While it thus possible that the smallest angle in BM_n can be an arbitrarily small improvement of α_1, we show, as part of the following theorem, that this can only occur at one vertex and under a very specific circumstance. The following theorem details the worse case limits of angle improvement generally. Its proof provides insight into the mechanisms of angle improvement resulting from Delaunay insertion.

Theorem 3.1 *a) Angle $CP_1M \ge \alpha_0$ and the other two angles of triangle CP_1M exceed $\alpha_{min}(M)$. (See (9) for $\alpha_{min}(M)$.)*

b) Angle $MP_{NA-1}A \ge \alpha_1$ and the other two angles of triangle $MP_{NA-1}A$ exceed $\alpha_{min}(M)$.

c) If $NA > 2$, then in the set of triangles $P_jP_{j+1}M$ for $1 \le j \le NA - 2$, every angle exceeds $\alpha_{min}(M)$.

Proof: To establish this result, we will look at an algorithm for constructing the partial cavity of M and use it to trace the evolution of new angles in BM_n.

S is a stack of triangles initialized by CDA, the neighbour of triangle t_A on edge CA
while S is not empty **do**
1. $t = \mathrm{pop}(S)$; (removes t from S)
if $M \in CC(t)$ **then**
2. t is in the partial cavity of M

3. identify vertices of t as Q_0, Q_1, Q_2 of t labeled so that M is on the side of edge Q_0Q_2 opposite to Q_1

if 4. t has a neighbouring triangle on edge Q_0Q_1 **then**
push it onto S
end if
if t has a neighbouring triangle on edge Q_1Q_2 **then**
push it onto S
end if
5. Swap edge Q_0Q_2 with edge Q_1M in the quadrilateral $Q_0Q_1Q_2M$
end if
end while

When the algorithm terminates the partial cavity of M has been converted to BM_n.

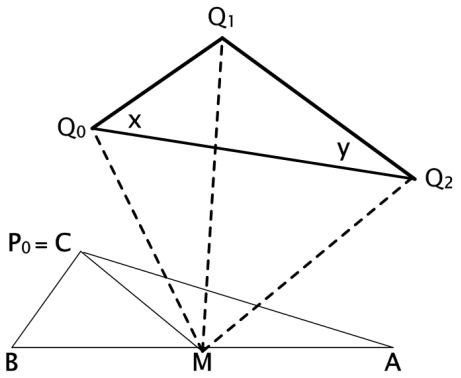

Figure 11: Configuration of quadrilateral Q_0, Q_1, Q_2, M for Theorem 3.1

When the edge swap step is entered, the quadrilateral $Q_0Q_1Q_2M$ is configured as in Figure 11; M is in $CC(Q_0Q_1Q_2)$. The effect on the angles at the vertices of this quadrilateral are:

at Q_0 Angle $Q_1Q_0Q_2$ is denoted by x in Figure 11. Evidently $x \geq \alpha_{min}(M)$ so angle x is replaced at Q_0 by $MQ_0Q_2 + x \geq MQ_0Q_2 + \alpha_{min}(M)$

at Q_2 As at Q_0, $MQ_2Q_0 = y$ is replaced at Q_2 by $MQ_2Q_0 + y \geq MQ_2Q_0 + \alpha_{min}(M)$

at Q_1 By the symmetry of circumcircles, Q_1 is inside $CC(MQ_0Q_2)$. Angles Q_0Q_1M and Q_0Q_2M subtend the same chord, Q_0M, of $CC(MQ_0Q_2)$. So, Q_1 inside this circle implies that angle $Q_0Q_1M >$ angleQ_0Q_2M. Similarly, $Q_2Q_1M \geq$ angleQ_2Q_0M

at M Angles Q_0MQ_1 and $Q_0Q_2Q_1$ subtend the same chord of $CC(Q_0Q_1Q_2)$. So, M inside this circle implies that angle $Q_0MQ_1 >$ angle$Q_0Q_2Q_1 \geq \alpha_{min}(M)$. Similarly, $Q_2MQ_1 >$ angle$Q_2Q_0Q_1 \geq \alpha_{min}(M)$.

So, the angles at M always exceed $\alpha_{min}(M)$.

There are two angles at each P_j, $1 \leq j \leq NA-1$, angle MP_jP_{j-1}, and angle MP_jP_{j+1}. Angle $MP_jP_{j-1} \geq m\alpha_{min}(M)$, where m is the number of times P_j is identified as Q_2 in step 3. of the algorithm, and similarly for angle MP_jP_{j+1}. What about MP_jP_{j+1} for $j = 0$, i.e. MCP_1? Angle

$MP_0P_1 = MCP_1$ and angle $t_A = \alpha_0$ share the chord CA of $CC(t_A)$. From Lemma 3.1 we know P_1 is in $CC(t_A)$; so we can conclude that $MP_0P_1 > \alpha_O$. Similarly, angle $MP_{NA-1}A$ and angle MCA both share chord AM of $CC(T_A)$; so angle $MP_{NA-1}A > \alpha_1$. □

Corollary 3.1 *If t is obtuse, then no new angles smaller than the existing ones in the unrefined mesh result from Delaunay terminal edge refinement of t*

3.2 non-terminal CA

If the partial cavity of M is the trivial one consisting of only t_A, then the prospects of mesh improvement by Delaunay insertion do not apply to t_A. In this case, if α_0 is small, then this angle is still in the mesh, in t_A. When CA is not a terminal edge in the mesh, removing α_0 from the mesh can be accomplished by removing the edge CA through subsequent refinements. In this subsection, we study some special instances in which it can be shown that CA is not a terminal edge of t_A and its neighbour, $t_{A,2}$, on edge CA.

Lemma 3.2 *If BC is the shortest edge of t_B, then edge CA is not a terminal edge of t_A if*

$$\alpha_0(t_{A,2}) < \pi - 2arctan(3tan(\alpha_0)) \tag{10}$$

Proof: Theorem 2.3 implies that CA is not a terminal edge of the mesh if

$$\alpha_0(t_{A,2}) < 2\alpha_2 - \pi \tag{11}$$

We develop a lower bound for α_2 to prove the lemma. Without additional assumptions, the only lower bound on α_2 would be $\pi/2$, which occurs when C lies on the bisector of edge AB. If this lower bound is place into the right hand side of (11), the result is 0, and no useful information results. Figure 12 shows t, but not t_A or t_B. The midpoint, M of edge AB is marked and so is the quarter

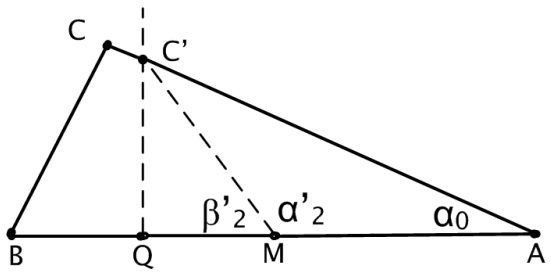

Figure 12: for Lemma 3.2

point Q which is the midpoint of edge BM of t_B. The condition that BC is the shortest edge of t_B implies that C lies to the left of the vertical line through Q, shown in the figure as dashed; it intersects edge CA at C'. Evidently, the angle, $AMC' = \alpha_2'$ is a minimum for α_2 wherever C lies. We show that

$$\alpha_2' = \pi - arctan(3\,tan(\alpha_0)\,) \tag{12}$$

as follows.

$$\begin{aligned} |C' - Q| &= |Q - M| \, tan(\beta_2') = \frac{|B - A|}{4} tan(\beta_2') \\ |C' - Q| &= |Q - A| \, tan(\alpha_0) = \frac{3|B - A|}{4} tan(\alpha_0) \end{aligned}$$

so $tan(\beta_2') = 3tan(\alpha_0)$ i.e. $\beta_2' = arctan(3tan(\alpha_0))$. Since $\alpha_2' + \beta_2' = \pi$, (12) follows.

Since α_2' is a lower bound for α_2, Theorem 2.3 implies that CA is not a terminal edge unless $\alpha_2(t_{A,2}) > 2\alpha_2' - \pi$. The lemma then follows by substituting (12) into this expression. □ .

Corollary 3.2 *If $\alpha_0 \leq \pi/6$ and edge BC is the shortest edge of t_B, then edge CA is not terminal.*

Proof: : $\pi - arctan(3\,tan(\alpha_0))$ is monotone decreasing in α_0. If $\alpha_0 \leq \pi/6$, then

$$\alpha_{-2} => \pi - arctan(3\,tan(\pi/6))$$

But $\pi - arctan(3\,tan(\pi/6)) = 2\pi/3$ since $tan(\pi/6) = 1/sqrt(3)$ and $arctan(sqrt(3)) = \pi/3$. But, as Figure 12 shows, α_{-2} ia a lower bound for α_2 and, by Theorem 2.2, CA cannot be a terminal edge of t_A if $\alpha_2 > 2\pi/3$ □ .

Corollary 3.3 *If $\alpha_0 < \pi/4.4$ and edge BC is the shortest edge of t_B, then CA is not terminal, unless $\alpha_0(t_2) > \alpha_0$*

Proof: $\pi - arctan(3\,tan(\alpha_0))$ is monotone decreasing in α_0. Equation $x = \pi - arctan(3\,tan(x))$ has its unique solution at $\bar{x}$ just below $\pi/4.4$. So for $\alpha_0 < \pi/4.4$,

$$\alpha_0 < \bar{x} = \pi - arctan(3\,tan(\bar{x})) < \pi - arctan(3\,tan(\alpha_0)).$$

So if $\alpha_0(t_2) \leq \alpha_0$, then the lemma shows that edge CA cannot be terminal □ .

3.3 Small edge improvement

In this section, we show that if t is shaped so that $|B - C| < |C - M|$, i.e. if $|B - C|$ is the shortest edge of t_B, then Delaunay insertion of M into the mesh can only produce new edges that are longer than $|B - C|$. We then look at repeated Deter applied to a special case of t.

Figure 13 shows the terminal triangle ABC, and an arc of its circumcircle $CC(ABC)$. The point C' is the projection of C onto edge BA. The figure also shows the insertion point M, and an arc of $CC(T_A)$. We assume that $|C - M| > |A - M|$, and consequently, that t is acute and that $\alpha_1 < \alpha_0$. The line CD_b is parallel to edge BA. D_b is the point of intersection of this line with $CC(T_A)$ and N_{lim} is the midpoint of line segment CD_b. The point C_{im} is the point of intersection of $CC(ABC)$ and line segment CD_b.

Lemma 3.3 *If $|C - M| > |B - C|$, the circle of radius $|B - C|$ about M lies inside $CC(ABC)$*

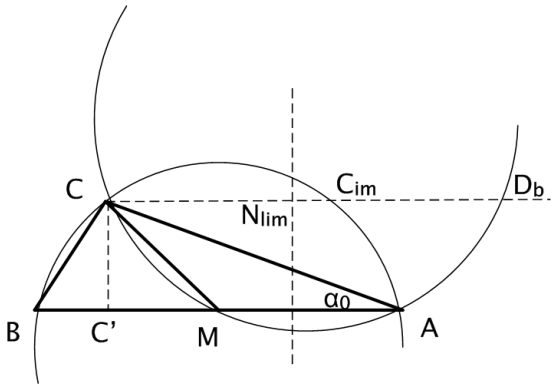

Figure 13: Configuration of terminal triangle t and its neighbour

Proof Introduce coordinates (r, s) with origin at B and r axis along edge BA[4]. Let the coordinates of A be $(z, 0)$ and the coordinates of C be (a, b). Then $|B - C|^2 = a^2 + b^2$ which we will denote by d^2. Then (r, s) on the circle of radius $|B - C|$ about M satisfies

$$(r - z/2)^2 + s^2 = d^2. \tag{13}$$

The equation for $CC(ABC)$ is

$$(r - z/2)^2 + (s - c)^2 = z^2/4 + c^2. \tag{14}$$

where

$$c = (d^2 - az)/(2b). \tag{15}$$

Note that the centre of $CC(ABC)$ lies on the bisector of edge AB. Let $(z/2, \bar{s})$ be the point of maximum height of $CC(ABC)$ above AB. The coordinate form of the condition $|C - M| > |B - C|$ is $a < z/4$. We want to show that if this condition holds, we have $d < \bar{s}$. Suppose the contrary holds, i.e. $\bar{s}^2 < d^2$. Then, using (14),

$$2c\bar{s} + z^2/4 < d^2$$

or

$$\bar{s} < (d^2 - z^2/4)/2c$$

Using (15), this implies $\bar{s} < f\, b$ for $f = (d^2 - z^2/4)/(d^2 - az)$. However, if $a < z/4$, this implies $f < 1$, i.e. $(s) < b$, which is impossible, since $\bar{s}$ is the maximum height of $CC(ABC)$. Consequently, $a < z/4$ is incompatible with $\bar{s}^2 < d^2$. □

Corollary 3.4 *If $|B - C|$ is the shortest edge of t_B then Delaunay insertion of M into the current mesh can only produce edges longer than $|B - C|$.*

We now use this lemma in a theorem that demonstrates a special case of t_A for which we can prove that no new small edges are produced in repeated Deter refinements of t. Let D be the vertex of the triangle, $t_{A,2}$, that shares edge CA with t_A. D must be outside $CC(ABC)$.

[4]These are longest edge coordinates, See Simpson [30]

Theorem 3.2 *If $\alpha_0 \leq \alpha_0(t_{A,2})$, and $|B-C|$ is the shortest edge of t_B, and edge CA is not a terminal edge of t_A, then the circle of radius $|B-C|$ about M is empty for repeated applications of Deter refinement to t_A.*

Proof: Note that edge CD must lie on, or above line CD_b because angle $ACD = \alpha_0(t_{A,2})$, is not smaller than α_0. There are two cases to consider. The first case is that D is inside $CC(t_A)$. In this case, there is a non trivial partial cavity of M. Then Lemma 3.3 proves the result, since D lies outside $CC(ABC)$.

In the second case, D is on or outside $CC(t_A)$, and t_A is the trivial partial cavity of M. Then, since CA is not a terminal edge, there are two subcases for the Deter refinement process applied to t_A. In subcase 1, as a result of $Lepp(t_A)$, Deter refinement inserts a point above edge CD that lies in $CC(t_{A,2})$. This removes edge CD and no small edge at M occurs. In subcase 2, CD is bisected - perhaps several times - until the midpoint, N, of one of the bisections lies inside $CC(t_A)$. Then N must lie between N_{lim} and D_b. But $|M - N_{lim}| > |B-C|$ so $|N - M > |B-C|$, even though N can be inside $CC(ABC)$. □ It may be interesting to note that if the relation on the minimum angles of t_A and $t_{A,2}$ of this theorem were reversed, i.e. $\alpha(t_{A,2}) < \alpha_0 < \pi/4.4$, and edge BC is the shortest edge of t_B, then it follows from Corollary 3.3 that CA cannot be a terminal edge.

References

[1] M. Berzins, Mesh Quality: A Function of Geometry, Errror Estimates or Both?, *Engineering with Computers*, 15, 1999, 236-247.

[2] M. Bern, D. Eppstein and J. Gilbert, Provably good mesh generation. *Journal Computer System Science*, 48, 1994, 384–409.

[3] L. Paul Chew. Guaranteed-quality mesh generation for curved surfaces. In *Proc. 9th Annual Comp. Geometry*. ACM Press, 1993.

[4] P L George and H Borouchaki, *Delaunay Triangulation and Meshing*. Hermes, 1998.

[5] H Borouchaki and P L George, Aspects of 2-D Delaunay Mesh Generation. *International Journal for Numerical Methods in Engineering*, **40**, 1997, 1957-1975.

[6] R.E.Bank, *PLTMG: A Software Package for Solving Elliptic Partial Differential Equations, Users' Guide 8.0*. SIAM, 1998.

[7] M. C. Rivara, Algorithms for refining triangular grids suitable for adaptive and multigrid techniques, *International Journal for Numerical Methods in Engineering*, **20**, 1984, 745–756.

[8] M. C. Rivara. Selective refinement/derefinement algorithms for sequences of nested triangulations. *International Journal for Numerical Methods in Engineering*, **28**, 1989, 2889–2906.

[9] M. C. Rivara and C. Levin. A 3d Refinement Algorithm for adaptive and multigrid Techniques. *Communications in Applied Numerical Methods*, **8**, 1992, 281–290.

[10] P Morin, R H Nochetto, and K G Siebert, Convergence of Adaptive Finite Element Methods, *SIAM Review*.**44**, 2002, 631-658.

[11] S. N. Muthukrishnan, P. S. Shiakolos R. V. Nambiar, and K. L. Lawrence. Simple algorithm for adaptative refinement of three-dimensional finite element tetrahedral meshes. *AIAA Journal*, **33**, 1995, 928–932.

[12] N. Nambiar, R. Valera, K. L. Lawrence, R. B. Morgan, and D. Amil. An algorithm for adaptive refinement of triangular finite element meshes. *International Journal for Numerical Methods in Engineering*, **36**, 1993, 499–509.

[13] M. C. Rivara and M. Venere. Cost Analysis of the longest-side (triangle bisection) Refinement Algorithms for Triangulations. *Engineering with Computers*, **12**, 1996, 224–234.

[14] M. C. Rivara and G. Iribarren, The 4-triangles longest-edge partition of triangles and linear refinement algorithms, Mathematics of Computation, 65, 1996, 1485-1502.

[15] M. C. Rivara. New longest-edge algorithms for the refinement and/or improvement of unstructured triangulations. *International Journal for Numerical Methods in Engineering*, **40**, 1997, 3313–3324.

[16] J Ruppert. A Delaunay refinement algorithm for quality 2-dimensional mesh generation. *J. of Algorithms*, **18**, 1995, 548–585.

[17] N. Hitschfeld and M.C. Rivara. Automatic construction of non-obtuse boundary and/or interface Delaunay triangulations for control volume methods. *International Journal for Numerical Methods in Engineering*, **55**, 2002, 803–816.

[18] N. Hitschfeld, L. Villablanca, J. Krause, and M.C. Rivara. Improving the quality of meshes for the simulation of semiconductor devices using Lepp-based algorithms. *to appear. International Journal for Numerical Methods in Engineering*, 2003.

[19] M. C. Rivara, N. Hitschfeld, and R. B. Simpson. Terminal edges Delaunay (small angle based) algorithm for the quality triangulation problem. *Computer-Aided Design*, **33**, 2001, 263–277.

[20] M. C. Rivara and M. Palma. New LEPP Algorithms for Quality Polygon and Volume Triangulation: Implementation Issues and Practical Behavior. *In Trends unstructured mesh generation*, Eds: S. A. Cannan . Saigal, AMD, **220**, 1997, 1–8.

[21] T.J. Baker, Automatic mesh generation for complex three dimensional regions using a constrained Delaunay triangulation. *Engineering with Computers*, **5**, 1989, 161-175.

[22] T. J. Baker, Triangulations, Mesh Generation and Point Placement Strategies. *Computing the Future,* ed. *D Caughey*,John Wiley, 61-75.

[23] R E Bank and A H Sherman. The use of adaptive grid refinement for badly behaved elliptic partial differential equations. In R Vichnevetsky and R S Stepleman, editors, *Advances in Computer Methods for Partial Differential Equations- III*, pages 33–39. IMACS, 1979.

[24] G Sewell. A finite element program with automatic user-controlled mesh grading. In R Vichnevetsky and R S Stepleman, editors, *Advances in Computer Methods for Partial Differential Equations- III*, pages 8–10. IMACS, 1979.

[25] J R Shewchuk, Triangle: Engineering a 2D Quality Mesh Generator and Delaunay Triangulator. *First Workshop on Applied Computational Geometry*, ACM, 1996, 124-133.

[26] J R Shewchuk. What is a good linear element? interpolation, conditioning, and quality measures. In S Owen, editor, *Proceedings: 11th International Meshing Round Table*. Sandia National Laboratories, 2002.

[27] R.B. Simpson, N. Hitschfeld and M.C. Rivara, Approximate quality mesh generation, *Engineering with computers*, **17**, 2001, 287-298.

[28] M.C. Rivara and N. Hitschfeld,LEPP-Delaunay algorithm: a robust tool for producing size-optimal quality triangulations, *Proc. of the 8th Int. Meshing Roundtable*, October 1999, 205-220.

[29] R.B. Simpson, Anisotropic Mesh Transformations and Optimal Error Control. *Applied Numerical Mathematics*, **14**, 1994, 183-198.

[30] R.B. Simpson, Geometry Independence for a Meshing Engine for 2D Manifolds. *International Journal for Numerical Methods in Engineering*, **60**, 2004, 675-694.

[31] M. Bern, Triangulations, In Handbook of Discrete and Computational Geometry *J. E. Goodman and J O'Rourke (eds.), CRC Press Boca Raton*, 1997.

[32] D. T. Lee and A. Lin Generalized Delaunay triangulation for planar graphs. *Disc and Comp Geom*, bf 1, 1986, 201-217.

[33] N.P. Weatherill and O. Hassan, Efficient three-dimensional Delaunay triangulation with automatic point creation and imposed boundary constraints. *IJMNE*, bf 37, 1994, 2005-2039.

[34] D.L. Marcum and N.P. Weatherill, Aerospace applications of solution adaptive finite element analysis. *CAGEOD*, bf 12, 1995, 709-731

[35] I.G. Rosenberg and F. Stenger, A lower bound on the angles of triangles constructed by bisecting the longest side, Mathematics of Computation, 29, 1975, 390-395.